# **Enhanced Mechanical and Acoustic Performance of Layered Metal-Mesh Eucalyptus Multi-ply Structures**

Yan Qiu,<sup>a</sup> Chen Chen,<sup>a,b</sup> and Wei Xu a,\*

The mechanical and acoustic performances of five-layer eucalyptus plywood reinforced with copper and stainless steel meshes were studied, focusing on the effects of mesh type, layer count, and mesh size. Experimental results demonstrated that incorporating metal mesh significantly enhanced both mechanical properties and acoustic vibration characteristics. The mechanical performance peaked at two-layer reinforcement configurations, with static elastic modulus values reaching 8,570 MPa (copper) and 9,100 MPa (steel), while mesh size exhibited negligible influence. Acoustic metrics, including acoustic conversion efficiency (ACE) and specific dynamic elastic modulus (Esp), also achieved optimal values in two-layer composites, with copper outperforming steel (e.g., ACE: 248 vs. 213). Notably, copper composites exhibited superior vibrational energy retention, with a minimum loss tangent of 0.0259, compared to 0.0246 for steel. The findings highlight that layer count, rather than mesh size or type, dominated performance optimization. Two-layer configurations balanced interfacial stress distribution and bonding efficiency, yielding the highest mechanical and acoustic outputs. These metal-reinforced composites offer sustainable alternatives to traditional tonewoods reducing reliance on endangered species while enabling cost-effective utilization of low-grade timber. Their enhanced acoustic-mechanical synergy positions them as promising materials for musical instruments, home audio systems. This work provides actionable insights for eco-friendly material design in industrial and musical applications.

DOI: 10.15376/biores.20.4.9962-9979

Keywords: Metal-wood composites; Acoustic vibration properties; Static/dynamic elastic modulus; Sustainable tonewoods; Layer-dependent optimization

Contact information: a: College of Furnishings and Industrial Design, Nanjing Forestry University Nanjing, Jiangsu, China; b: Zhejiang Moganshan Home Furnishing Co., Ltd, Zhejiang, China; \*Corresponding author: xuwei@njfu.edu.cn

#### INTRODUCTION

Music, as an integral component of human culture, has always held a significant position throughout China's long history. From its role as a core element of ancient "elegant culture" to its widespread development in modern society, music not only reflects the inheritance and evolution of culture but also profoundly influences people's daily lives (Calvano *et al.* 2023). Due to its unique acoustic properties, including sound absorption, resonance, and sound propagation, wood plays an irreplaceable role in musical instrument manufacturing. Manufacturers have also leveraged the improvement of wood's acoustic properties to address issues such as reverberation and sound pressure in residential spaces, thereby enhancing sound transmission performance and improving comfort within home

environments (Negro *et al.* 2017; Karaçali 2021; Salpriyan *et al.* 2025). In recent years, with the growing demand for modern acoustic applications, enhancing the acoustic properties of wood has garnered significant attention, particularly in the fields of musical instruments, home audio systems, and architectural acoustics.

The selection of wood and its manufacturing processes determine the quality of musical instruments. Manufacturers typically choose wood having exceptional acoustic properties, which exhibit excellent dimensional stability, uniform texture, flexibility, and workability (Bucur 2017; Sproßmann *et al.* 2017). Tropical hardwoods are commonly used in instrument production due to their superior acoustic performance (Holz 1996). However, many tropical hardwoods are now facing issues of overexploitation. For example, Brazilian rosewood and certain species of mahogany are protected under the Convention on International Trade in Endangered Species of Wild Fauna and Flora (CITES) (Pfriem 2015). As a result, high-quality wood for instrument manufacturing has become increasingly scarce and expensive (Torres *et al.* 2015). Consequently, there is a growing demand for alternatives to tropical hardwoods in instrument production. This has led to an urgent need to identify sustainable substitute materials. One promising approach is the use of physical, chemical, and biological treatments to enhance the functional properties of fast-growing plantation wood, enabling it to match the acoustic performance of high-quality tropical hardwoods (Chung *et al.* 2017).

Experiments aimed at improving wood properties for replacing traditional tonewoods have primarily focused on physical and chemical methods. High-temperature thermal treatment of wood enhances its hydrophobicity and dimensional stability, thereby improving its acoustic performance (Rowell 2013; Kang et al. 2016; Zhu et al. 2017). Additionally, many researchers have employed chemical modifications, such as acetylation, impregnation, and oil heat treatment, to achieve superior sound quality and stable acoustic properties (Roohnia et al. 2011; Ilyich et al. 2016; Liu et al. 2020). Furthermore, significant efforts have been directed toward the development of wood-based composite materials as alternatives to traditional solid wood for musical instruments, addressing the issue of wood resource scarcity. Wood-based composites, which combine wood matrices with reinforcing materials, exhibit enhanced properties that overcome the limitations of natural wood while allowing for tailored modifications based on specific application requirements (Maloney 1996; Gardner et al. 2015; Papadopoulos 2019). Researchers have conducted experiments combining various reinforcing materials with wood to investigate changes in acoustic performance indices. For instance, Santoni et al. (2020) developed a wood-plastic composite (WPC) by combining natural fiber-filled polymers with wood flour and optimized the sound transmission loss of WPC panels using numerical methods. They performed vibroacoustic analyses on orthotropic WPC plates, examining the effects of structural connections and boundary conditions on acoustic performance (Santoni et al. 2020). Liu et al. (2019) studied the sound insulation and mechanical properties of medium-density fiberboard (MDF) and rubber multilayer composite panels. By optimizing hot-pressing parameters, temperature, and adhesive content, they combined MDF with rubber materials, demonstrating that the sound insulation efficiency and mechanical performance of the multilayer composites significantly improved with increasing rubber thickness (Liu et al. 2019). Hillig et al. (2024) utilized non-destructive testing methods, such as ultrasonic and stress wave propagation, to evaluate the bending strength and stiffness of WPCs. Their results revealed a correlation between mechanical properties (strength and stiffness) and wave velocity as well as stiffness coefficients (Hillig et al. 2024). Matsubara et al. (2000) proposed a numerical model accounting for the heterogeneity of composite laminates, stacking fiberboards and matrix boards to validate the effectiveness of their modeling approach. The experimental results confirmed the potential of composites as viable substitutes for traditional tonewoods (Matsubara et al. 2000). Hao et al. (2023) conducted experiments combining metal mesh with birch veneer to investigate the influence of metal mesh layers on the acoustic vibration properties of the composites. Their findings indicated that the acoustic vibration characteristics of the composites met general musical instrument requirements, offering excellent dimensional stability and serving as a promising alternative to traditional solid wood soundboards (Hao et al. 2023).

These studies highlight the potential of composite materials in acoustic applications. Compared to high-quality tonewoods, such as those required for high-end instruments, composites offer lower costs and higher strength. Different types of composites can enhance specific acoustic properties, making them viable alternatives for traditional wooden instruments, home audio systems, and other applications (Damodaran et al. 2015; Ribeiro et al. 2021; Mohammed and Meincken 2023). However, research on the preparation of metal-wood composite materials via veneer lamination for application in musical instrument soundboards remains relatively limited. Metals, as common reinforcing phases in composites, have attracted significant attention due to their high strength, high modulus, excellent dimensional stability, aging resistance, and superior thermal and electrical conductivity (Hu et al. 2010). By combining metals and wood, the synergistic advantages of both materials can be fully utilized while effectively mitigating their inherent limitations (Mohebby et al. 2011). Such composites demonstrate great potential in functional applications, including conductive materials and electromagnetic shielding (Xia et al. 2017), offering new perspectives for the design and development of high-performance materials.

Metal meshes, such as copper and stainless steel, are particularly advantageous as reinforcing materials in composites. Copper mesh is renowned for its excellent electrical conductivity, thermal conductivity, and corrosion resistance, while stainless-steel mesh exhibits high strength, high modulus, and outstanding aging resistance. These properties enable metal meshes to significantly enhance the mechanical and functional performances of composites. Eucalyptus wood, as a lightweight plies material with a high elastic modulus and inherent acoustic properties, features a unique fiber structure that forms strong interfacial bonds with metal meshes, thereby optimizing the overall performance of the composite. Meanwhile, due to its anatomical structure, eucalyptus wood often develops fine-scale cracks during drying, which may adversely affect its acoustic performance. This issue can be mitigated by incorporating a continuous metal mesh. Therefore, experiments combining copper mesh and stainless-steel mesh with eucalyptus wood to investigate improvements in mechanical and acoustic properties are of significant value. Such composites not only meet the comprehensive requirements of acoustic materials for lightweight design, high strength, and acoustic performance, but they also provide new insights for the design and development of novel acoustic functional materials.

This study further investigated the composite materials formed by combining copper mesh and stainless-steel mesh with eucalyptus wood. It explored the effects of mesh layer count, mesh size, and mesh type on the mechanical and acoustic properties of the composite, aiming to optimize the composite structure for use as a substitute for tonewoods and acoustic materials in furniture, such as sound systems. The research aimed to enhance the acoustic vibration characteristics of the material.

### **EXPERIMENTAL**

# **Test Materials and Equipment**

Eucalyptus veneer was used as the wood ply material. The veneer was dried naturally to achieve a moisture content of approximately 8% to 12%. The surface of the veneer was cleaned to remove dust and dirt, followed by light sanding or sandblasting to increase surface roughness, ensuring stability during the composite fabrication process. The veneer was then cut into dimensions of 350 mm × 350 mm. Formaldehyde-free soybean adhesive was prepared according to the ratio used in actual production of composite wood by Zhejiang Moganshan Home Furnishing Co., Ltd. The adhesive mixture consisted of 30 g of high-temperature soybean flour, 20 g of low-temperature soybean flour, 56 g of water, and 44 g of polyamide-epichlorohydrin resin (PAE) per 150 g of adhesive. Copper mesh and stainless-steel mesh (40,80,120 mesh), with a purity of 99.999%, were used as reinforcing materials. The mesh, with an original size of 2000 mm × 1050 mm × 0.1 mm, was cut into 350 mm × 350 mm × 0.1 mm pieces, with a wire diameter of 0.006 mm.

**Table 1.** Experimental Materials

Material	Dimensions/Purity	Supplier	
Eucalyptus Veneer	350 mm×350 mm×2.5 mm	Zhejiang Moganshan Home Furnishing Co., Ltd.	
Copper Mesh (40, 80, 120 mesh)	350 mm×350 mm×0.1 mm	Yuqian Metal Materials Co., Ltd., Qinghe County	
Stainless-steel Mesh (40, 80, 120 mesh)	350 mm×350 mm×0.1 mm	Yuqian Metal Materials Co., Ltd., Qinghe County	
Low-temperature Soybean Flour	99%	Zhejiang Moganshan Home Furnishing Co., Ltd.	
High-temperature Soybean Flour	99%	Zhejiang Moganshan Home Furnishing Co., Ltd.	
Polyamide-epichlorohydrin Resin (PAE)	99%	Zhejiang Moganshan Home Furnishing Co., Ltd.	

**Table 2.** Experimental Facilities

Instrument Name	Model	Manufacturer
Hot presses	XLB-D	Huzhou Shunli Rubber Machinery Co., Ltd.
Magnetic Stirring Water Bath	HH-4J	Changzhou Langyue Instrument Manufacturing Co., Ltd.
Electronic Universal Testing Machine	UTM6000	Shenzhen Sansi Zongheng Technology Co., Ltd.
Fast Fourier Transform (FFT) Spectrum Analyzer	CF-9200	ONO Sokki, Japan
Signal Generator	DG1022Z	Rigol Technologies Co., Ltd.
Magnetic Excitation Actuator	DH41020	Jiangsu Donghua Testing Technology Co., Ltd.
Laser Doppler Vibrometer	ENV-RID- AVD1	Hefei Fuhuang Junda High-Tech Information Technology Co., Ltd.
Electronic Scale	1	Yangzhou Mailaote Experimental Instrument Co., Ltd.

All experimental procedures were conducted in accordance with the Chinese National Standard GB/T 17657-2022, "Test Methods for Evaluating the Properties of Wood-Based Panels and Surface Decorated Wood-Based Panels." The experimental materials and equipment are listed in Table 1 and Table 2, respectively.

# **Experimental Material Preparation**

After preparing the soybean adhesive, it was evenly applied along the wood grain using a brush, employing a single-sided adhesive application method. The adhesive application rate for veneer-to-veneer bonding was controlled at 220 to 230 g/m², while the application rate for the sides of the veneer in contact with the metal mesh was increased to 300 to 310 g/m². The reinforcing materials and eucalyptus veneer were assembled in a cross-grain configuration, as illustrated in Fig. 1. The five-layer eucalyptus veneer structure included four interfaces, labeled as layers 1, 2, 3, and 4. Metal mesh reinforcing materials were placed between layers 1 and 4 to create metal mesh-wood composite panels. The number of metal mesh layers varied from 1 to 4, resulting in samples labeled A-D. For example, a composite with one metal mesh layer placed at layer 1 was labeled A1, while a composite with one metal mesh layer placed at layer 2 was labeled A2. Composites with two metal mesh layers were labeled as follows: B1 (layers 1 and 2), B2 (layers 1 and 3), B3 (layers 1 and 4), and B4 (layers 2 and 3). Composites with three metal mesh layers were labeled C1 (layers 1, 2, and 3) and C2 (layers 1, 2, and 4). Finally, a composite with four metal mesh layers was labeled D1.

The composite materials were then processed using a hot presses under the following conditions: a hot-pressing temperature of 120 °C, a hot-pressing time of 20 min, and a hot-pressing pressure of 1.2 MPa. After cooling and stabilizing, the composite materials were cut into 300 mm × 300 mm specimens for mechanical and acoustic testing.

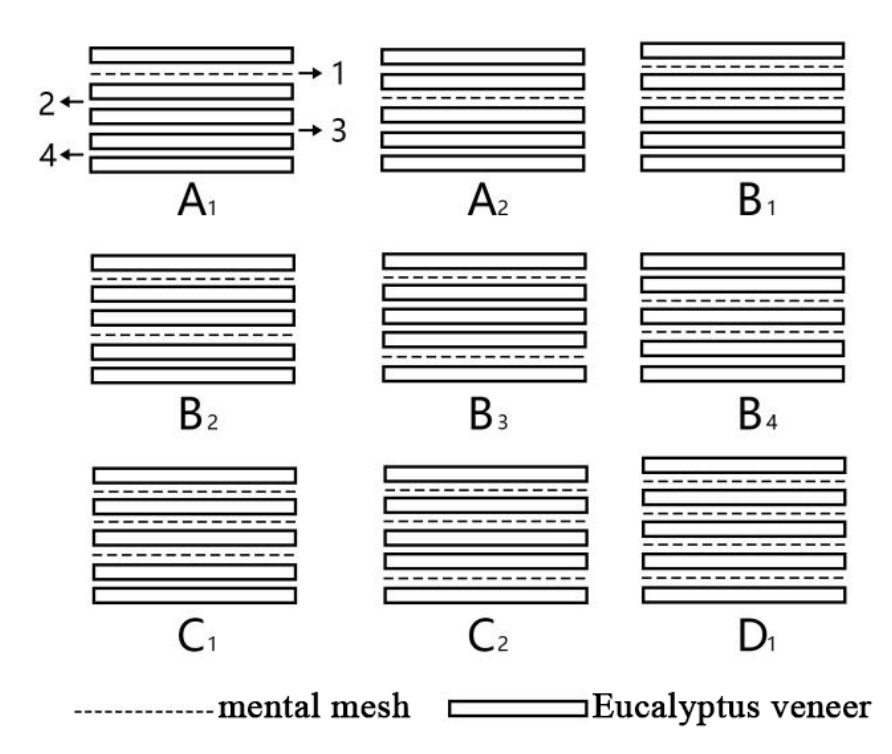


Fig. 1. Schematic diagram of the five-layer metal-mesh reinforced composite structure

# **Bonding Strength Test**

The bonding strength of the composite materials was tested using an electronic universal testing machine. In accordance with GB/T 17657-2022, the composite specimens were prepared with a length of 100 mm and a width of 25 mm, where the grain orientation of the wood was in the transverse direction. The shear surface length of the specimens was 13 mm, and the notch depth was cut to two-thirds of the core thickness during specimen preparation. The specimens were immersed in hot water at  $(63 \pm 3)$  °C for 3 h, removed, and then cooled at room temperature for 10 minutes. Subsequently, the specimens were placed in the movable fixture of the testing machine. An appropriate loading speed was selected, and a constant loading rate was applied to ensure that the specimens failed within  $(30 \pm 10)$  seconds. The maximum load value was recorded with an accuracy of 10 N. The bonding strength of the specimens was calculated using the following formula,

$$X_A = \frac{P_{max}}{b \times l} \times 0.9 \tag{1}$$

where  $X_A$  represents the bonding strength of the specimen, measured in MPa;  $P_{\text{max}}$  denotes the maximum failure load (N); b is the width of the shear surface (mm); and l is the length of the shear surface (mm).

#### Static Elastic Modulus Test

In accordance with GB/T 17657-2022, the static elastic modulus was tested using an electronic universal testing machine. Composite specimens were cut to dimensions of 300 mm (length)  $\times$  20 mm (width) and positioned horizontally on supports, with their longitudinal axis perpendicular to the support rollers and the center aligned beneath the loading roller. The elastic modulus ( $E_{\rm b}$ ) was calculated using the following formula, with results rounded to the nearest 10 MPa,

$$E_{\rm b} = \frac{l_1^3}{4 \times b \times t^3} \times \frac{F_2 - F_1}{a_2 - a_1} \tag{2}$$

where  $E_{\rm b}$  is the elastic modulus (MPa);  $l_1$  represents the span between supports (mm); t is specimen thickness (mm);  $F_2 - F_1$  is load increment within the linear region (10% to 40% of maximum load), measured in newtons (N); and  $a_2 - a_1$  is the corresponding mid-span deflection increment (mm).

#### Acoustic Performance Test

Based on the vibration theory of beams under free-free boundary conditions, the acoustic vibration properties of wood were measured using a Fast Fourier Transform (FFT) spectrum analyzer. A magnetic sheet was attached to the bottom of one end of the specimen, which was then suspended horizontally by two thin strings. The distances from the two suspension points to the respective ends of the specimen were both 0.224 times its length. An electromagnetic shaker was positioned directly beneath the magnetic sheet to provide vibration excitation. The sensor was positioned above the end of the specimen, close to but not in contact with the specimen (Qian *et al.* 2023). An ultrasonic instrument was used to induce vibrations at the other end of the specimen, and the resulting vibration signals were processed using FFT to generate the vibration spectrum, as shown in Fig. 2. Based on the vibration spectrum, the following acoustic vibration performance parameters were calculated: dynamic elastic modulus, specific dynamic elastic modulus, sound radiation quality constant, acoustic impedance, dynamic shear modulus, logarithmic

decrement, loss tangent, and acoustic conversion efficiency (Bucur 2023). All resonance frequencies utilized in this experiment corresponded to the first-order resonance frequencies of the specimens.

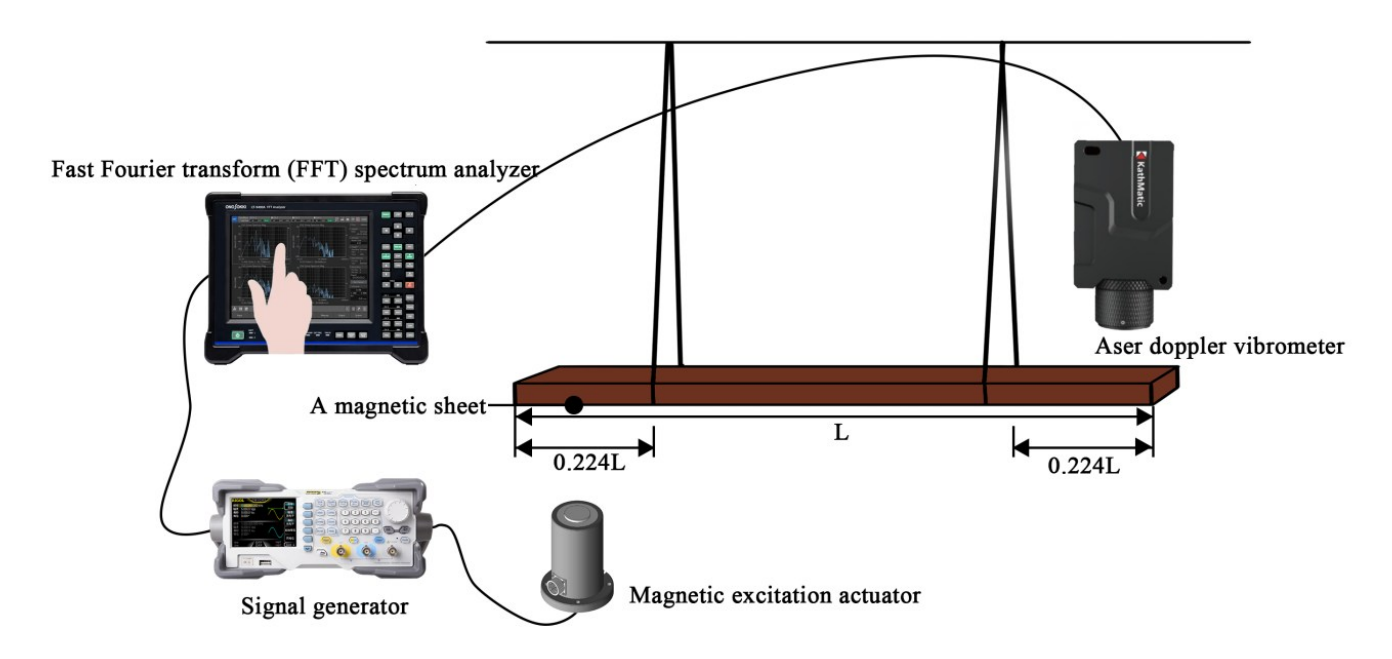


**Fig. 2.** Schematic diagram of Fast Fourier Transform (FFT) spectrum analyzer setup for vibration testing

Dynamic elastic modulus

The dynamic elastic modulus was calculated as,

$$E = \frac{48\rho\pi^2 l^4}{h^2 m^4 10^6} f_n^2 \tag{3}$$

where E is the dynamic elastic modulus of the specimen (GPa);  $\rho$  is the density of the specimen (kg/m³); l is the length of the specimen (m); h is the thickness of the specimen (m);  $f_n$  is the n-th natural frequency of the specimen (Hz); m is a parameter determined by the boundary conditions.

Specific dynamic elastic modulus

The specific dynamic elastic modulus ( $E_{sp}$ ) represents the vibration acceleration per unit cell wall mass of wood, where higher values indicate superior vibrational efficiency.

$$E_{\rm sp} = E/\rho \tag{4}$$

In Eq. 4,  $E_{\rm sp}$  is the specific dynamic elastic modulus of the specimen (GPa).

Sound radiation quality constant

The parameter R quantifies the acoustic power radiated to the surrounding air. Tonewoods are typically selected based on their high values of R.

$$R = \frac{v}{\rho} = \sqrt{\frac{E}{\rho^3}} \tag{5}$$

In Eq. 5, R is the sound radiation quality constant of the specimen (mPa<sup>-1</sup>· s<sup>-3</sup>).

Acoustic impedance

The acoustic impedance was calculated as,

$$\omega = \sqrt{E\rho} \tag{6}$$

where  $\omega$  is the acoustic impedance of the specimen (Pa· s·m<sup>-1</sup>)

#### Logarithmic decrement

The logarithmic decrement characterizes vibrational damping, with lower values preferred for tonewoods to minimize energy loss and enhance sustain,

$$\delta = \frac{1}{n} \ln \frac{A_1}{A_n} \approx \tan \delta \times \pi \tag{7}$$

where  $\delta$  is the logarithmic decrement of the specimen; and  $A_1$ ,  $A_n$  are the amplitudes of the first and n-th cycles of the time-domain sinusoidal wave, respectively.

## Loss tangent

The loss tangent characterizes vibrational damping, with lower values preferred for tonewoods to minimize energy loss and enhance sustain:

$$\tan \delta \approx \delta / \pi \tag{8}$$

Acoustic conversion efficiency

The ACE reflects the material's ability to convert vibrational energy into sound energy, with higher values indicating superior conversion performance:

$$ACE = \frac{\sqrt{E/\rho^3}}{\tan \delta} \tag{9}$$

#### RESULTS AND DISCUSSION

## **Bonding Strength Analysis**

The bonding performance of the composites was investigated using a universal testing machine. Composites with varying metal mesh layers were compared to a control group of five-layer eucalyptus veneer composites. For each composite type, 16 specimens were prepared and tested in accordance with the Chinese National Standard GB/T 17657-2022. The bonding strength of different adhesive layers was evaluated, with a threshold value >1 MPa indicating compliance with the standard.

As shown in Table 3, the results demonstrated that while the addition of metal mesh reinforcement slightly reduced the bonding strength of the composites—particularly in the adhesive layers containing metal—all tested values remained compliant with the national standard. This reduction is attributed to the interfacial stress concentration caused by the metal mesh, yet the overall performance satisfied the requirements for structural integrity in acoustic material applications.

Composite Type	Bonding Strength (MPa)	SD	Composite Type	Bonding Strength (MPa)	SD
Copper Mesh (40 mesh, 1L)	1.42	0.065	Steel Mesh (40 mesh, 1L)	1.50	0.040
Copper Mesh (40 mesh, 2L)	1.41	0.082	Steel Mesh (40 mesh, 2L)	1.57	0.078
Copper Mesh (40 mesh, 3L)	1.36	0.063	Steel Mesh (40 mesh, 3L)	1.39	0.055
Copper Mesh (40 mesh, 4L)	1.31	0.046	Steel Mesh (40 mesh, 4L)	1.41	0.047
Copper Mesh (80 mesh, 1L)	1.32	0.072	Steel Mesh (80 mesh, 1L)	1.34	0.043
Copper Mesh (80 mesh, 2L)	1.28	0.084	Steel Mesh (80 mesh, 2L)	1.52	0.079
Copper Mesh (80 mesh, 3L)	1.25	0.044	Steel Mesh (80 mesh, 3L)	1.25	0.032
Copper Mesh (80 mesh, 4L)	1.26	0.057	Steel Mesh (80 mesh, 4L)	1.22	0.048
Copper Mesh (120 mesh, 1L)	1.23		Steel Mesh (120 mesh, 1L)	1.23	
Copper Mesh (120 mesh, 2L)	1.24		Steel Mesh (120 mesh, 2L)	1.58	
Copper Mesh (120 mesh, 3L)	1.23		Steel Mesh (120 mesh, 3L)	1.22	
Copper Mesh (120 mesh, 4L)	1.19		Steel Mesh (120 mesh, 4L)	1.37	
Control (No metal mesh)	1.73		<u> </u>		

**Table 3.** Bonding Strength of Composite Materials

# **Static Elastic Modulus Analysis**

The static elastic modulus of the composites was tested using a universal testing machine to evaluate the effects of metal mesh type, layer count, and mesh size on the mechanical properties of the wood composites. For each composite configuration, six specimens per composite type were tested, and the results were averaged. As shown in Fig. 3, the static elastic modulus of stainless-steel mesh composites varied depending on the adhesive layer configuration, exhibiting an initial increase followed by a decrease. The highest modulus was observed in composites with two steel mesh layers. Among the four two-layer configurations, the average static elastic modulus values were 6,950 MPa (40 mesh), 7,690 MPa (80 mesh), and 8,360 MPa (120 mesh). Notably, the mesh size had minimal impact on the static elastic modulus, with no clear correlation observed. For two-layer configurations, the highest modulus values were achieved in the B4 composite structure (Table 4), reaching 8,570 MPa (40 mesh), 7,950 MPa (80 mesh), and 9,100 MPa (120 mesh).

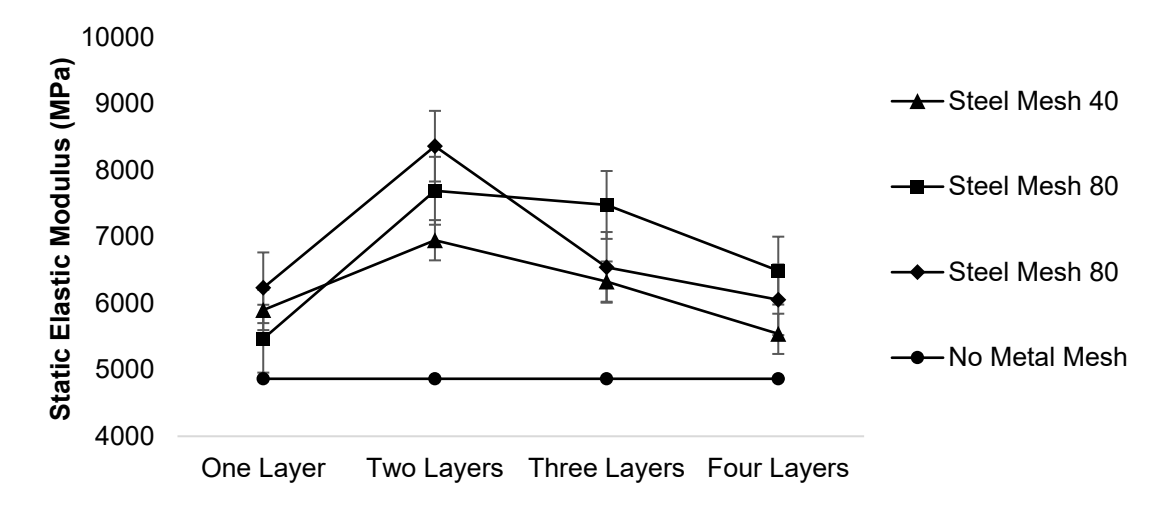


Fig. 3. Static elastic modulus of steel composites

Composite Configuration	40 Mesh	80 Mesh	120 Mesh
B1	6280	7350	6570
B2	4880	7800	8790
B3	8070	7660	8990
B4	8570	7950	9100

**Table 4.** Static Elastic Modulus of Two-Layer Steel Composites (MPa)

As illustrated in Fig. 4, the static elastic modulus of copper mesh composites also demonstrated a non-monotonic trend, peaking at two layers. The average values for two-layer copper composites were 7,570 MPa (40 mesh), 7,430 MPa (80 mesh), and 7,710 MPa (120 mesh). For two-layer configurations, the B3 composite structure yielded the highest modulus values: 8,080 MPa (40 mesh), 7,720 MPa (80 mesh), and 7,890 MPa (120 mesh).

The experimental data indicate that the type and mesh size of the metal reinforcement had negligible effects on the static elastic modulus, while the number of layers was the dominant factor. Both steel and copper composites exhibited peak performance at two layers. However, the optimal configurations differed: copper mesh composites achieved maximum mechanical performance when the reinforcement was placed in the outermost adhesive layer, whereas steel mesh composites performed best when the reinforcement was embedded in the innermost two adhesive layers.

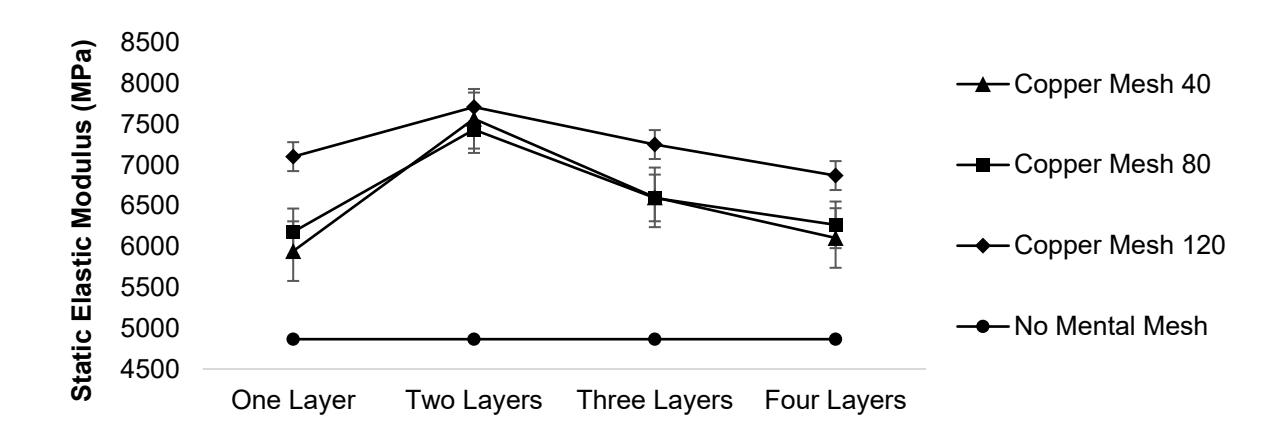


Fig. 4. Static elastic modulus of copper composites

**Table 5.** Static Elastic Modulus of Two-Layer Steel Composites (MPa)

Composite Configuration	40 Mesh	80 Mesh	120 Mesh
B1	7528	6879	7546
B2	7087	7655	7553
B3	8083	7723	7889
B4	7493	7476	7851

# **Acoustic Performance Analysis**

Acoustic vibration performance parameters, including dynamic elastic modulus (E), specific dynamic elastic modulus  $(E_{sp})$ , sound radiation quality constant (R), acoustic impedance  $(\omega)$ , logarithmic decrement  $(\delta)$ , loss tangent  $(\tan \delta)$ , and acoustic conversion efficiency (ACE), were calculated for the five-layer composites using the respective Eqs. 3

to 9. The specific dynamic elastic modulus ( $E_{\rm sp}$ ) represents the vibration acceleration per unit cell wall mass of wood, where higher values indicate superior vibrational efficiency. The sound radiation quality constant (R) quantifies the acoustic power radiated to the surrounding air, and tonewoods are typically selected for their high R values. The logarithmic decrement ( $\delta$ ) and loss tangent ( $\tan \delta$ ) characterize vibrational damping, with lower values preferred for tonewoods to minimize energy loss and enhance sustain. The ACE reflects the material's ability to convert vibrational energy into sound energy, with higher values indicating superior conversion performance (Wegst 2006).

As shown in Fig. 5, copper composites exhibited the highest ACE values: 236 (40 mesh, 2L), 244 (80 mesh, 1L), and 248 (120 mesh, 2L). Steel composites achieved lower values: 222 (40 mesh, 1L), 219 (80 mesh, 2L), and 213 (120 mesh, 1L). The results demonstrated that copper composites outperform steel composites in ACE. The ACE of the metal composites showed minimal correlation with mesh size and exhibited no significant trends, with layer count being the dominant influencing factor.

According to Table 6, the ACE values exhibited notable differences across mesh sizes and structural types. For copper meshes, the B3 structure yielded the maximum ACE value at 258 in the 40-mesh group, while the A1 structure achieved the highest values in both the 80-mesh and 120-mesh groups, with 247 and 219, respectively. For steel meshes, the A1 structure demonstrated the highest ACE values in the 40-mesh and 120-mesh groups (231 and 220, respectively), whereas the B2 structure showed the maximum ACE value in the 80-mesh group (230). These results indicate that the optimal structural configuration varied with mesh size and material type, with the A1 structure generally exhibiting superior performance, particularly in the steel-based composites.

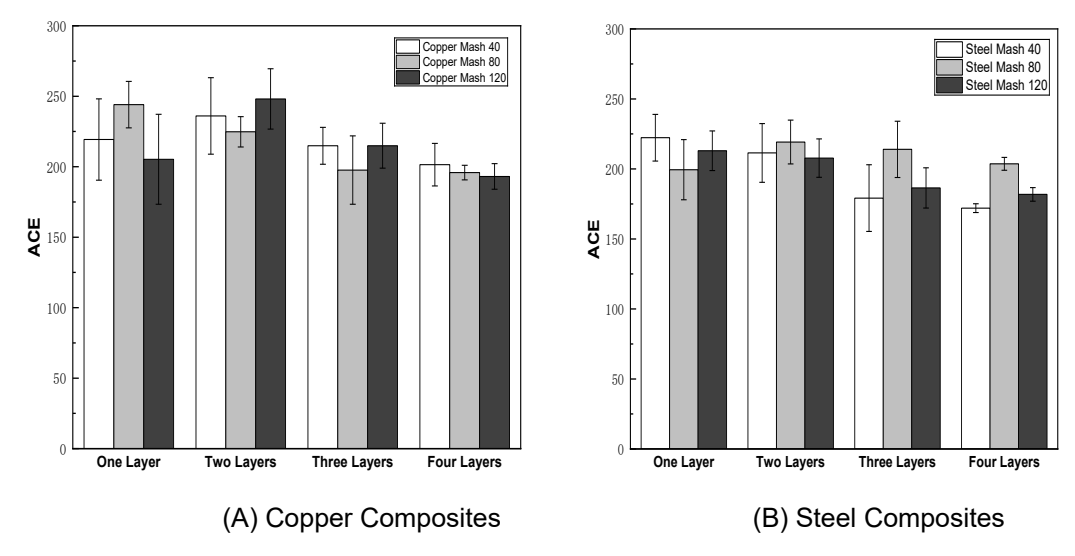


Fig. 5. Acoustic conversion efficiency of metal composites

	ACE	<b>A</b> <sub>1</sub>	$A_2$	B <sub>1</sub>	B <sub>2</sub>	B <sub>3</sub>	B <sub>4</sub>
	40 Mesh	/	/	240.91	196.44	257.80	248.97
Copper	80 Mesh	246.75	244.03	/	/	1	/
	120 Mesh	/	/	264.75	224.55	248.77	254.33
	40 Mesh	230.74	213.86	/	1	1	1
Steel	80 Mesh	/	/	227.89	229.66	200.09	220.41
	120 Mesh	219.63	206.32	/	1	1	/

Table 6. Acoustic Conversion Efficiency of Metal Composites

The specific dynamic elastic modulus ( $E_{\rm sp}$ ) represents the vibrational acceleration per unit cell wall mass of wood, where higher values indicate superior vibrational efficiency. As shown in Fig. 6, the highest  $E_{\rm sp}$  values for copper composites were achieved in two-layer reinforced structures: 16.8 (40 mesh), 15.8 (80 mesh), and 18.6 (120 mesh). Similarly, steel composites exhibited peak  $E_{\rm sp}$  values in two-layer configurations: 16.9 (40 mesh), 18.4 (80 mesh), and 17.6 (120 mesh). Comparative analysis revealed that the  $E_{\rm sp}$  of metal composites showed minimal dependence on mesh size, with performance predominantly governed by layer count. Both material types exhibited a non-monotonic trend, peaking at two layers. This suggests that the interaction between metal reinforcement and wood plies is optimized in intermediate-layer configurations, balancing stress distribution, and interfacial bonding.

According to Table 7, the maximum  $E_{\rm sp}$  value for copper 40-mesh was obtained in the B4 structure (17.4), while the B3 structure exhibited the highest  $E_{\rm sp}$  values in both the 80-mesh and 120-mesh groups, at 16.3 and 19.2, respectively. For steel meshes, the B4 structure achieved the highest  $E_{\rm sp}$  value in the 40-mesh group (19.0), the B1 structure yielded the maximum in the 80-mesh group (19.3), and the B4 structure again showed the highest value in the 120-mesh group (18.1). These findings suggest that the  $E_{\rm sp}$  performance is highly dependent on both mesh size and structural configuration, with B3 and B4 structures showing relatively superior results across multiple conditions.

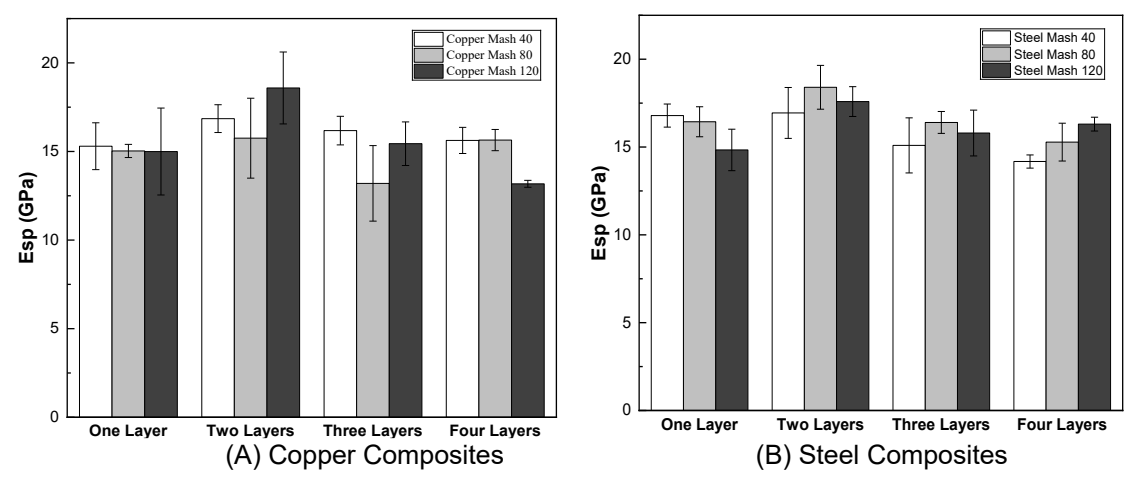


Fig. 6. Specific dynamic elastic modulus of metal composites

	$E_{sp}$	B <sub>1</sub>	B <sub>2</sub>	B <sub>3</sub>	B <sub>4</sub>
	40 Mesh	15.92	16.89	17.17	17.42
Copper	80 Mesh	15.32	15.67	16.31	14.21
	120 Mesh	17.31	18.44	19.21	18.96
Steel	40 Mesh	15.56	17.10	16.07	19.03
	80 Mesh	19.29	17.60	17.69	19.01
	120 Mesh	18.01	16.51	17.70	18.14

**Table 7.** Specific Dynamic Elastic Modulus of Metal Composites

The sound radiation quality constant (R) quantifies the acoustic power radiated from wood materials to the surrounding air. As shown in Fig. 7, the R values of metal composites exhibited trends consistent with their specific dynamic elastic modulus  $(E_{\rm sp})$  profiles (Fig. 6). Copper composites achieved the maximum R value of 7.00 in 120-mesh two-layer configurations, while steel composites peaked at 6.25 in 80-mesh two-layer structures. Statistical analysis confirmed the QQ values of copper composites demonstrated significant superiority over steel counterparts (P < 0.05, one-way ANOVA).

According to Table 7, the highest R values for copper meshes were observed in the B3 structure for both the 40-mesh (6.89) and 80-mesh (6.76) groups, while the B1 structure yielded the maximum R value in the 120-mesh group (7.25). For steel meshes, the B4 structure consistently exhibited the highest R values across all mesh sizes, with 5.84, 6.66, and 5.82 for the 40-, 80-, and 120-mesh groups, respectively. These results indicate that the B3 structure tends to perform best in copper-based composites, whereas the B4 structure dominates in steel-based composites regardless of mesh size.

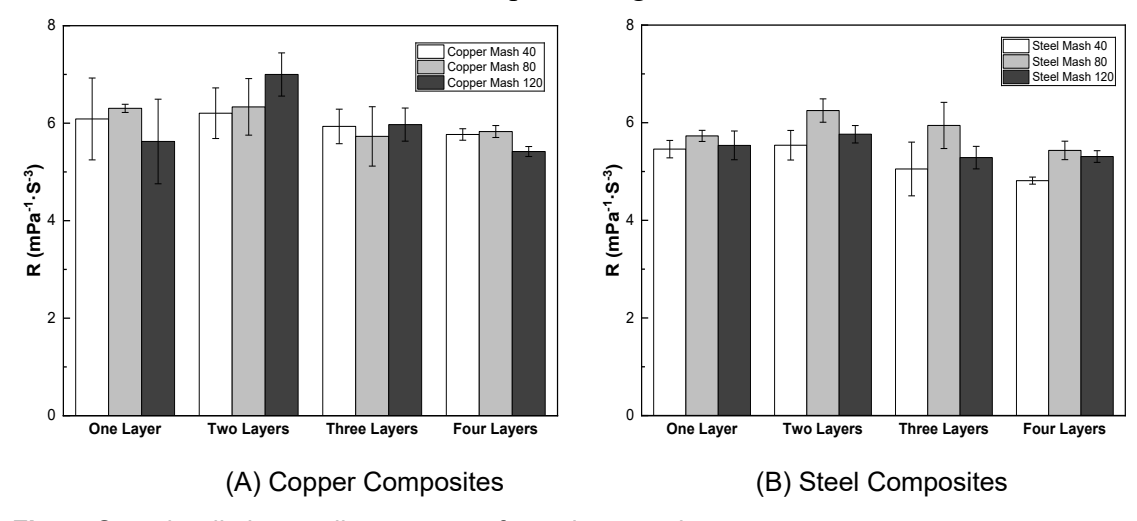


Fig. 7. Sound radiation quality constant of metal composites

 Table 8. Sound Radiation Quality Constant of Metal Composites

	R	B <sub>1</sub>	B <sub>2</sub>	B <sub>3</sub>	B <sub>4</sub>
	40 Mesh	6.25	5.59	6.89	6.10
Copper	80 Mesh	6.50	5.40	6.76	6.67
	120 Mesh	7.25	6.64	7.04	7.07
	40 Mesh	5.54	5.70	5.12	5.84
Steel	80 Mesh	5.98	6.48	6.29	6.66
	120 Mesh	5.81	5.61	5.81	5.82

The logarithmic decrement ( $\delta$ ) and loss tangent ( $\tan\delta$ ) characterize the vibrational damping properties of materials. Tonewoods are typically selected for their low  $\delta$  and  $\tan\delta$  values, as lower values minimize vibrational energy loss, enhance efficiency, and improve sustain in musical instruments. Copper and steel composites exhibited minimal variation in  $\tan\delta$  across mesh sizes, layer counts, and material types. The lowest  $\tan\delta$  values were observed in the 80-mesh single-layer copper composite (0.0259) and the 40-mesh single-layer steel composite (0.0246).

According to Table 7, the lowest  $\tan\delta$  value for copper 40-mesh was observed in the B4 structure (0.0287), while the A1 structure exhibited the minimum value in the 80-mesh group (0.0254) and the B1 structure in the 120-mesh group (0.0274). For steel meshes, the lowest  $\tan\delta$  values were obtained from the A1 structure in the 40-mesh group (0.0243), the D1 structure in the 80-mesh group (0.0267), and the A2 structure in the 120-mesh group (0.0259). These results suggest that the optimal structural configuration for minimizing energy dissipation varies with both mesh size and material type, with steel-based composites generally achieving lower  $\tan\delta$  values compared to copper-based composites.

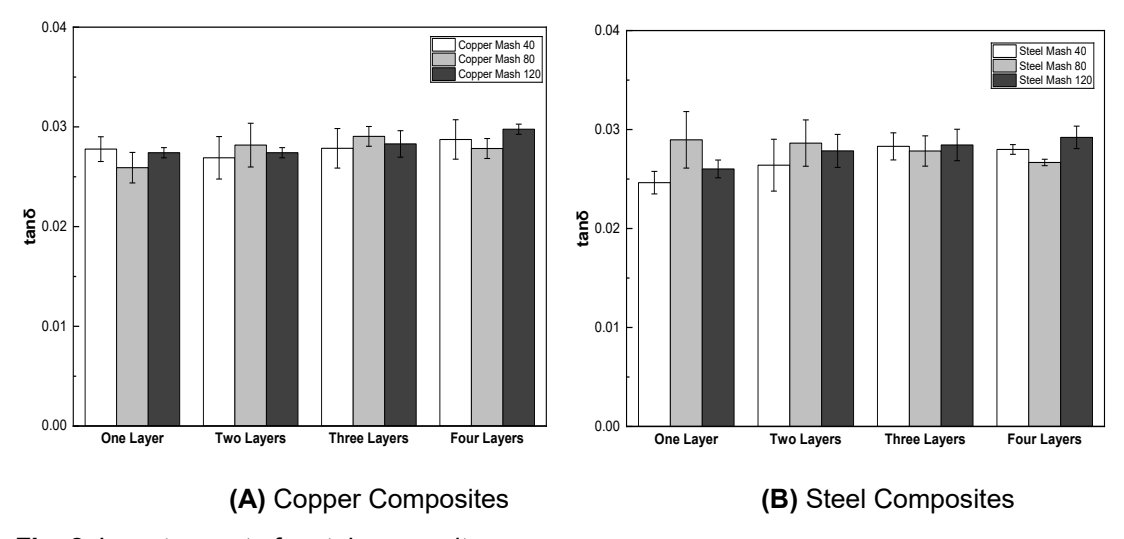


Fig. 8. Loss tangent of metal composites

**Table 9.** Loss Tangent of Metal Composites

	tanδ	A1	A2	B1	B2	В3	B4	D1
Copper	40 Mesh	1	1	0.0272	0.0285	0.0271	0.0247	/
	80 Mesh	0.0254	0.0259	/	/	/	1	/
	120 Mesh	/	1	0.0274	0.0296	0.0278	0.0285	/
	40 Mesh	0.0243	0.0249	/	/	/	/	/
Steel	80 Mesh	/	1	/	/	/	/	0.0267
	120 Mesh	0.0261	0.0259	/	/	/	/	/

According to the comparative results presented in Tables 6 to 9, the performance of metal mesh—wood veneer composites varied significantly with mesh size, material type, and structural configuration. For ACE values, the A1 structure generally exhibited superior performance, particularly in steel meshes, whereas copper meshes showed higher variability, with B3 performing best in the 40-mesh group. In terms of Esp values, the B3 and B4 structures demonstrated consistently higher performance in copper and steel

meshes, respectively, indicating their advantages in enhancing elastic storage capacity. For R values, the B3 structure dominated in copper meshes (40- and 80-mesh), while the B1 structure was optimal in the 120-mesh group; conversely, the B4 structure consistently achieved the highest R values across all steel meshes, suggesting its structural suitability for vibration resistance. With respect to damping performance, represented by  $\tan \delta$ , the optimal configurations differed more substantially, with A1, B1, B4, D1, and A2 structures alternately yielding the lowest values depending on mesh size and material, while steel-based composites generally exhibited lower  $\tan \delta$  values than their copper counterparts. Overall, these findings highlight that the optimal structural configuration is not universal but depends strongly on both mesh size and material type: B3 and A1 structures tend to enhance acoustic efficiency in copper-based composites, whereas B4 structures demonstrate more stable advantages in steel-based composites.

According to Hao (2023), the ACE,  $E_{\rm sp}$ , R, and  $\tan\delta$  values of Paulownia are 141, 12.6, 10.1, and 0.202, respectively. Although the eucalyptus—metal composites show some deficiency in terms of the R value, their performance in the other acoustic parameters is comparable to, or even surpasses, that of Paulownia. This suggests that eucalyptus—metal mesh composites can, to some extent, meet the requirements of musical soundboard materials.

#### CONCLUSIONS

The experimental investigation into copper- and steel-reinforced eucalyptus composites revealed critical insights into the interplay between material composition, structural configuration, and acoustic-mechanical performance. All mechanical and acoustic tests were conducted in the transverse direction relative to the wood grain (*i.e.*, in the plane of the board), ensuring consistency across measurements. Key findings demonstrate the following:

- 1. Layer-Count Dominance: The number of reinforcement layers exerts greater influence on both mechanical and acoustic properties than mesh size or material type. Two-layer configurations consistently achieved peak performance, with copper composites exhibiting superior acoustic conversion efficiency (ACE = 248.10) and sound radiation quality constant (R = 6.9998), outperforming steel counterparts by 16.5% and 12.0%, respectively.
- 2. Material-Specific Advantages: Copper composites demonstrated enhanced vibrational energy retention, evidenced by lower loss tangent values ( $\tan \delta = 0.0259$ ) compared to steel ( $\tan \delta = 0.0246$ ). This damping superiority, coupled with copper's ductility, enables efficient energy transduction, particularly in high-mesh configurations (120 mesh).
- 3. Mesh Size Insensitivity: Variations in mesh density (40 to 120 mesh) induced marginal fluctuations in performance, confirming that interfacial bonding quality—rather than pore geometry—governs energy transfer dynamics.

4. Sustainable Acoustic Material Potential: With ACE, R, and  $\tan\delta$  values exceeding traditional tonewoods such as Sitka spruce wood (ACE =141, R =12.63,  $\tan\delta$  =0.2024), copper composites present a viable eco-friendly alternative for musical instrument soundboards and architectural acoustics, reducing reliance on endangered hardwoods while utilizing low-grade timber.

#### REFERENCES CITED

- Bucur, V. (2017). "Acoustics of wood," Materials Science Forum 210, 101-108.
- Bucur, V. (2023). "A review on acoustics of wood as a tool for quality assessment," *Forests* 14(8), article 1545. DOI: 10.3390/f14081545
- Calvano, S., Negro, F., Ruffinatto, F., Zanuttini-Frank, D., and Zanutini, R. (2023). "Use and sustainability of wood in acoustic guitars: An overview based on the global market," *Helivon* 9(4), article e15218. DOI: 10.1016/j.heliyon.2023.e15218
- Chung, H., Park, Y., Yang, S. Y., Kim, H., Han, Y., Chang, Y. S., and Yeo, H. (2017). "Effect of heat treatment temperature and time on sound absorption coefficient of *Larix kaempferi* wood," *Journal of Wood Science* 63, 575-579. DOI: 10.1007/s10086-017-1662-z
- Damodaran, A., Lessard, L., and Suresh Babu, A. (2015). "An overview of fibre-reinforced composites for musical instrument soundboards," *Acoustics Australia* 43, 117-122. DOI: 10.1007/s40857-015-0008-5
- Gardner, D. J., Han, Y., and Wang, L. (2015). "Wood–plastic composite technology," *Current Forestry Reports* 1, 139-150. DOI: 10.1007/s40725-015-0016-6
- GB/T 17657-2022. "Test methods for the physical and chemical properties of wood-based panels and surfaced wood-based panels," Standardization Administration of China, Beijing, China.
- Hao, Q. (2023). "Preparation and acoustic vibration performance of birch veneer-metal composites," Master's thesis, *Northeast Forestry University*. DOI: 10.27009/d.cnki.gdblu.2023.000412.
- Hao, Q., Wang, Y. D., Ge, Y., Zhou, J., and Liu, Z. B. (2023). "Acoustic vibration properties of birch veneer-copper mesh composite," *Journal of Beijing Forestry University* 45(1), 148-158. DOI: 10.12171/j.1000-1522.20220378
- Hillig, É., Bobadilla, I., Arriaga, F., and Íñiguez-González, G. (2024). "Using acoustic testing to estimate strength and stiffness of wood-polymer composites," *Maderas. Ciencia y Tecnología* 26. DOI: 10.22320/s0718221x/2024.04
- Holz, D. (1996). "The acoustics of wood," CRC Press. DOI: 10.1201/9780203710128
- Hu, Y. C., Li, J., Cheng, F. C., and Zhang, X. J. (2010). "Design and property analysis of the metal mesh reinforced LVL," *Advanced Materials Research* 113, 2145-2149. DOI: 10.4028/www.scientific.net/AMR.113-116.2145
- Ilyich, F. V., Yurevna, S. E., Mikhailovna, T. E., and Savelevna, C. E. (2016). "Resonance wood microstructure peculiarities," *Wood Research* 61(3), 413-422.
- Kang, H. Y., Kang, C. W., Hong, S. H., and Matsumura, J. (2016). "Effect of heat treatment on the acoustic properties of a wooden xylophone keyboard," *Journal of the Faculty of Agriculture* 157-163. DOI:10.5109/1564098
- Karaçali, Ö. (2021). "Physical acoustics analysis of composite wooden panel and room by computational modeling," *Acta Physica Polonica A* 139(5), 483-486.

- Liu, M., Peng, L., Lyu, S., and Lyu, J. (2020). "Properties of common tropical hardwoods for fretboard of string instruments," *Journal of Wood Science* 66, 1-11. DOI: 10.1186/s10086-020-01862-7
- Liu, M., Peng, L., Fan, Z., and Wang, D. (2019). "Sound insulation and mechanical properties of wood damping composites," *Wood Res* 64(4), 743-758. DOI: 10.3390/ma13214964
- Maloney, T. M. (1996). "The family of wood composite materials," *Forest Products Journal* 46(2), article 18.
- Matsubara, T., Nishiwaki, T., and Maekawa, Z. (2000). "Design of FRP material substitutes for musical instrument," *Sen'i Kikai Gakkaishi (Journal of the Textile Machinery Society of Japan)* 53(11), T225-T231. DOI: 10.4188/transjtmsj.53.11 T225
- Mohammed, A. S., and Meincken, M. (2023). "Thermal and acoustic insulation properties of wood plastic composites (WPCs) for interior housing applications," *European Journal of Wood and Wood Products* 81(2), 421-437. DOI: 10.1007/s00107-022-01897-1
- Mohebby, B., Tavassoli, F., and Kazemi-Najafi, S. (2011). "Mechanical properties of medium density fiberboard reinforced with metal and woven synthetic nets," *European Journal of Wood and Wood Products* 69(2), 199-206. DOI: 10.1007/s00107-010-0412-3
- Negro, F., Cremonini, C., and Fringuellino, M. (2017). "An innovative composite plywood for the acoustic improvement of small closed spaces," *Holzforschung* 71(6), 521-526. DOI: 10.1515/hf-2016-0122
- Papadopoulos, A. N. (2019). "Advances in wood composites," *Polymers* 12(1), article 48. DOI: 10.3390/polym12010048
- Pfriem, A. (2015). "Thermally modified wood for use in musical instruments," *Drvna Industrija* 66(3), 251-253. DOI: 10.5552/drind.2015.1426
- Qian, H., Yida, W., Ying, G., Jing, Z., and Zhenbo, L. (2023). "Acoustic vibration performance of birch veneer-metal copper mesh composites," *Journal of Beijing Forestry University* 45(1), 148-158. DOI: 10.12171/j.1000-1522.20220378
- Ribeiro, R. S., Amlani, A. M., de Conto, J., Schwerz, B. G., Amarilla, R. S. D., Sant'Ana, L. H., and Matoski, A. (2021). "Acoustical treatment characterization of a classroom with wood-based composites," *Applied Acoustics* 178, article 107967. DOI: 10.1016/j.apacoust.2021.107967
- Roohnia, M., Hashemi-dizaji, S., Brancheriau, L., Tajdini, A., Hemmasi, A. H., and Manouchehri, N. (2011). "Effect of soaking process in water on the acoustical quality of wood for traditional musical instruments," *BioResources* 6(2), 2055-2065.
- Rowell, R. M. (2013). "Acoustical properties of acetylated wood," *Journal of Chemistry and Chemical Engineering* 7, 9,
- Salpriyan, P. M., Krishna, K., and Singh, T. (2025). "Recent developments in natural fibre polymer composite materials for interior design applications: an overview from acoustic perspective," *International Journal on Interactive Design and Manufacturing* (IJIDeM) 19(3),1563-1589. DOI: 0.1007/s12008-024-01935-7
- Santoni, A., Bonfiglio, P., Fausti, P., Marescotti, C., Mazzanti, V., and Pompoli, F. (2020). "Characterization and vibro-acoustic modeling of wood composite panels," *Materials* 13(8), article 1897. DOI: 10.3390/ma13081897

- Sproßmann, R., Zauer, M., and Wagenführ, A. (2017). "Characterization of acoustic and mechanical properties of common tropical woods used in classical guitars," *Results in Physics* 7, 1737-1742. DOI: 10.1016/j.rinp.2017.05.006
- Torres, J. A., and Torres-Martínez, R. (2015). "Evaluation of guitars and violins made using alternative woods through mobility measurements," *Archives of Acoustics* 40(3), 351-358. DOI: 10.1515/aoa-2015-0038
- Wegst, U. G. K. (2006). "Wood for sound," American *Journal of Botany* 93(10), 1439-1448. DOI: 10.3732/ajb.93.10.1439
- Xia, C., Yu, J., Shi, S. Q., Qiu, Y., Cai, L., Wu, H. F., and Zhang, H. (2017). "Natural fiber and aluminum sheet hybrid composites for high electromagnetic interference shielding performance," *Composites Part B: Engineering* 114, 121-127. DOI: 10.1016/j.compositesb.2017.01.044
- Zhu, L. J., Jiang, T., and Wu, G. (2017). "Improvement of acoustic-vibration performance of *E. urophylla* by high-temperature heat treatment," *Instrumentation and Automation* ICMIA 2017, 148-153. DOI: 10.2991/icmia-17.2017.26

Article submitted: July 12, 2025; Peer review completed: August 16, 2025; Revised version received: August 21, 2025; Accepted: August 31, 2025; Published: October 1, 2025.

DOI: 10.15376/biores.20.4.9962-9979